

Numerical Analysis of Jet Breakup Behavior Using Particle Method

Kazuya SHIBATA^{1*}, Seiichi KOSHIZUKA^{2*}, Yoshiaki OKA^{3*} and Toyoaki YAMAUCHI^{4*}

^{*1,2,3}*Nuclear Engineering Research Laboratory, The University of Tokyo,
2-22, Shirane, Shirakata, Tokai-mura, Naka-gun, Ibaraki-ken, 319-1188, Japan*

^{*4}*The Japan Atomic Power Company
1-1, Mitoshiro-tyo, Chiyoda-ku, Tokyo, 101-0053, Japan*

A continuous jet changes to droplets where jet breakup occurs. In this study, two-dimensional numerical analysis of jet breakup is performed using the MPS method (Moving Particle Semi-implicit Method) which is a particle method for incompressible flows. The continuous fluid surrounding the jet is neglected. Dependencies of the jet breakup length on the Weber number and the Froude number agree with the experiment. The size distribution of droplets is in agreement with the Nukiyama-Tanasawa distribution which has been widely used as an experimental correlation. Effects of the Weber number and the Froude number on the size distribution are also obtained.

KEYWORDS: *Jet breakup, Nukiyama-Tanasawa distribution, Breakup length, droplet size distribution, Weber number, Froude number.*

I. Introduction

Jet breakup is important for nuclear reactor safety. In severe accidents in light water reactors, molten core jets will be dispersed in a water pool and this process affects the subsequent phenomena, such as vapor explosions and the molten core coolability¹⁾. In sodium-cooled fast breeder reactors, high-pressure water is released into sodium as jets when the tubes are broken in the steam generators. Jet breakup also appears in many engineering problems: fuel injection into engines, inkjet printers, chemical plants, etc. The jet breakup length was experimentally investigated by Ricou and Spalding²⁾ for turbulent jets, Tanasawa and Toyoda³⁾, Grant and Middleman⁴⁾ for laminar and turbulent jets, Saito et al.⁵⁾ and Park et al.⁶⁾ for jet penetration with boiling. Kolev⁷⁾ reviewed correlations of the jet breakup length. The droplet size distribution after the jet breakup was experimentally obtained, for example, by Nukiyama and Tanasawa⁸⁾.

In order to analyze the jet breakup, we need a numerical method which can be used for disintegration of liquids as well as large deformation of free surfaces. This is not easy at the moment. Thus, most of analyses for engineering purposes employed experimental or theoretical correlations of the jet breakup: for example, in Moriyama et al.⁹⁾. Vierow¹⁰⁾ reviewed the treatment of jet breakup in the codes for nuclear safety.

Disintegration of jets released from a nozzle was analyzed by Richard et al.^{11,12)} using volume-of-fluid (VOF) and continuous-surface-force (CSF) methods. A series of droplets were generated by the jet breakup. However, the generated droplet sizes were almost the same and the number of the droplets was not so much.

Moving Particle Semi-implicit (MPS) method uses particles with fully Lagrangian description^{13, 14)}. Grids are not necessary at all. Breaking waves involving fluid

disintegration and coalescence were calculated by the MPS method¹⁵⁾. Thus, it will be useful to analyze jet breakup. Three-dimensional analysis of jet penetration was calculated by the MPS method¹⁶⁾ and the jet behavior agreed well with the experiment of Park et al.⁶⁾. In this case, surface tension was neglected because the jet behavior was mainly determined by momentum of the jet. Nomura et al.¹⁷⁾ developed a particle model for surface tension based on the CSF model¹⁸⁾. Single droplet breakup was calculated by the MPS method and a critical Weber number was obtained. Shirakawa et al.¹⁹⁾ analyzed jet behavior in the tube rupture accident in a steam generator of a liquid metal-cooled fast breeder reactor. In their calculations, surface tension was modeled by potential between two particles.

In the MPS method, fragmentation of fluids was easily calculated. This is a specific advantage of the MPS method which is free from the grid distortion. However, physical validity has not been discussed for the fragmentation. Numerical analysis of jet breakup and subsequent behavior of disintegrated droplets is expected to provide an example to consider such validity.

In the present study, breakup of jets released from a nozzle is analyzed by the MPS method. The calculation geometry is x-y two dimensions. Surface tension is considered. The breakup length is compared with the experimental data with various Weber numbers and Froude numbers. The size distribution of the disintegrated droplets obtained in the calculation is fitted by existing formula. Validity of the disintegrated particles in the MPS method is considered.

^{*}1 Kazuya SHIBATA, Tel.+81-29-287-8433,
Fax. +81-29-287-8488, E-mail: kazuya@utnl.jp

II. Moving Particle Semi-implicit Method

1. Governing Equations

Mass and momentum conservation equations for incompressible flow are used in this study:

$$\frac{D\rho}{Dt} = 0 \quad (1)$$

$$\rho \frac{D\bar{u}}{Dt} = -\nabla P + \mu \nabla^2 \bar{u} + \rho \bar{g} + \sigma \kappa \delta(d) \bar{n} \quad (2)$$

The mass conservation equation is represented by the density being constant, while divergence of velocity is usually used in the finite volume method. Since fully Lagrangian description is employed in the MPS method, the convection terms are not explicitly written. Viscosity is neglected in the present calculation of jet breakup.

2. Particle Interaction Models

A particle interacts with its neighbors using the following weight function $w(r)$:

$$w(r) = \begin{cases} \frac{r_e - r}{r_e} & 0 \leq r < r_e \\ 0 & r_e \leq r \end{cases} \quad (3)$$

where r is the distance between two particles, and r_e is a finite distance for limiting the interactions (Fig.1).

Differential operators, such as gradient and Laplacian, are represented by the following particle interaction models using the weight function:

$$\langle \nabla \phi \rangle_i = \frac{Z}{n^0} \sum_{j \neq i} \left[\frac{\phi_j - \phi_i}{|\vec{r}_j - \vec{r}_i|^2} (\vec{r}_j - \vec{r}_i) w(|\vec{r}_j - \vec{r}_i|) \right] \quad (4)$$

$$\langle \nabla^2 \phi \rangle_i = \frac{2Z}{n^0 \lambda} \sum_{j \neq i} [(\phi_j - \phi_i) w(|\vec{r}_j - \vec{r}_i|)] \quad (5)$$

where d and n^0 are the number of spatial dimensions and particle number density, respectively. The particle number density has two meanings; one is the normalization factor of the weighted average and the other is the value proportional to the fluid density. Thus, the particle number density is required to be constant from the mass conservation equation (Eq.(1)). The constant is denoted by n^0 .

$$n_i = \sum_{j \neq i} w(|\vec{r}_j - \vec{r}_i|) = n^0 \quad (6)$$

In Eq.(5), parameter λ is written as

$$\lambda = \frac{\sum_{j \neq i} w(|\vec{r}_j - \vec{r}_i|) |\vec{r}_j - \vec{r}_i|^2}{\sum_{j \neq i} w(|\vec{r}_j - \vec{r}_i|)} \cong \frac{\int_V w(r) r^2 dv}{\int_V w(r) dv} \quad (7)$$

Differential operators in the governing equations are substituted by the above particle interaction models and then the governing equations are transformed to dynamic equations of particles. Grids are not necessary in this discretization process.

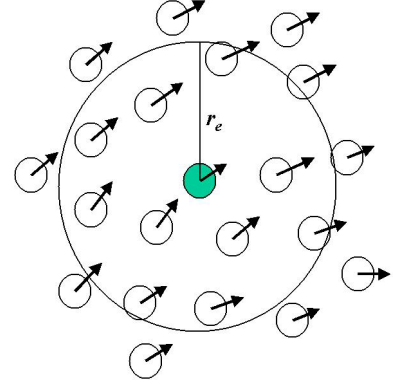


Fig.1 Particle interaction in weight function

3. Surface Tension Model

Surface tension is calculated at the particles on the free surface. We need to obtain curvature κ and unit normal vector \bar{n} at such particles (Fig.2). The particle number density is utilized for curvature.

$$\kappa = \frac{2 \cos \theta}{r_e^{st}} \quad (8)$$

$$2\theta = \frac{n_i^{st2}}{n_0^{st}} \pi \quad (9)$$

where the weight function used here is special for surface tension,

$$w^{st1}(r) = \begin{cases} 1 & 0 \leq r < r_e^{st} \\ 0 & r_e^{st} \leq r \end{cases} \quad (10)$$

$$w^{st2}(r) = \begin{cases} 1 & 0 \leq r < r_e^{st} \text{ and } n_j^{st1} > n_i^{st1} \\ 0 & \text{otherwise} \end{cases} \quad (11)$$

and $r_e^{st} = 3.1 l_0$. Particle number density n_i^{st1} is calculated by using Eq.(10) at first, and n_i^{st2} is then obtained by using Eq.(11).

In Eq.(9), a flat surface ($2\theta = \pi$) is assumed to be $n_i^{st2} = n_0^{st}$, which is estimated in advance in the initial particle configuration. Acute angles are obtained where $n_i^{st2} < n_0^{st}$, while obtuse angles are obtained where $n_i^{st2} > n_0^{st}$.

The unit normal vector is also calculated by utilizing the particle number density. Particle number densities at four positions near particle i are evaluated, $n_i^{\pm x}(\vec{r}_i \pm l_0 \bar{n}_x)$ and $n_i^{\pm y}(\vec{r}_i \pm l_0 \bar{n}_y)$ where \bar{n}_x and \bar{n}_y are unit vectors in x- and y-directions, respectively. The unit normal vector is calculated as,

$$\bar{a}_i = \frac{n_i^{+x} - n_i^{-x}}{2l_0} \bar{n}_x + \frac{n_i^{+y} - n_i^{-y}}{2l_0} \bar{n}_y \quad (12)$$

$$\bar{n}_i = \frac{\bar{a}_i}{|\bar{a}_i|} \quad (13)$$

Vector \bar{a}_i represents gradient of the particle number density around particle i . Smoothing of curvature is sometimes necessary for stability.

As shown in Fig.2, free surfaces have a thickness. Thus, we need to divide the calculated surface tension by the normalized thickness of d^{st}/l_0 . This model is based on the distribution of the particle number density because it

decreases toward the free surface. This idea is similar to the CSF model¹⁸⁾.

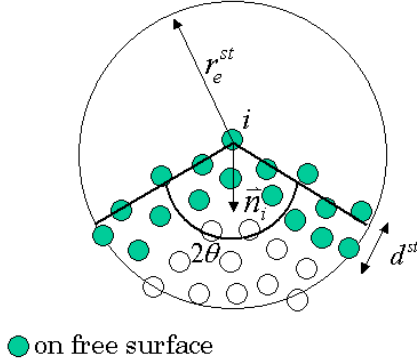


Fig.2 Particle model for surface tension

4. Algorithm for Incompressible Flow

A semi-implicit algorithm is employed in the MPS method; momentum conservation equations except for the pressure gradient term are explicitly solved in the first step, and the Poisson equation of pressure is implicitly solved in the second step. The Poisson equation of pressure is deduced from the implicit mass conservation equation and the implicit pressure gradient term.

The Poisson equation is discretized to a symmetric matrix equation using the Laplacian model (Eq.(5)). The matrix equation is solved by incomplete Cholesky decomposition conjugate gradient (ICCG) method.

The particle number density decreases toward the free surface because there are no particles outside. When the particle number density is below βn^0 , where $\beta = 0.95$, the particle is regarded as on the free surface. The Dirichlet boundary condition is applied to this particle in solving the Poisson equation of pressure.

III. Analysis of Jet Breakup Length

1. Calculation Condition

The calculation is two-dimensional. Figure 3 shows the schematic diagram of the calculation system. Non-viscous fluid is discharged downward from the nozzle. The width of the nozzle D is 0.013m, the density of the fluid is 1000kg/m³, and the spacing between the particles is 0.8125×10^{-3} m. It is verified that jet breakup length little change by the spacing between 1.3×10^{-3} m and 0.5×10^{-3} m.

The constant of particle number density n^0 for incompressibility condition is 6.540 ($r_e = 2.1l_0$). This constant is also used for judging free surface. The constant for calculating Laplacian of pressure Poisson equation n_0^{icg} is 35.61 ($r_e = 4.0l_0$). The constant for calculating surface tension n_0^{st} is 28.00 ($r_e = 3.1l_0$).

The nozzle is represented by fixed particles. New particles are generated at the inflow boundary that is the top of the nozzle. Outflow particles are eliminated at the outflow boundary that is the bottom of the calculation system. The initial particle arrangement is symmetry. There is no initial disturbance. Asymmetric disturbance may arise due to sequential calculation of the numerical algorithm. The continuous fluid surrounding the jet is

neglected. The definition of jet breakup length L is the length of the continuous part of the jet. In practice, jet breakup length is defined as the vertical distance between the outlet of the nozzle and the lowest part of the continuous jet. This length is average of 100 sampling data which are measured every 0.01 second. The condition of breakup is that the distance between droplets are more than four times of initial particle distance, where interactions between particles vanish in this model.

Calculations are performed by varying the surface tension coefficient and the fluid velocity. Dependencies on the Weber number (We) and the Froude number (Fr) are investigated. The definition of We and Fr are following.

$$We = \frac{\rho U^2 D}{\sigma}, \quad Fr = \frac{U}{\sqrt{gD}} \quad (14), (15)$$

Weber number expresses the ratio of inertial force to surface tension. Froude number expresses the ratio of inertial force to gravity.

In this study, the viscosity is neglected because the Ohnesorge number On which represents the effect of viscosity of droplet disintegration is about 0.001. In general, it is known that viscosity can be neglected if On is smaller than 0.1²⁰⁾.

2. Results and Discussion

Figure 4 shows the typical results. We can see the jet breakup in this figure. Jet shapes are not symmetrical. The reason is that ICCG solver was used for solving pressure Poisson equation. Calculation of fast solver such as ICCG and SOR is sequential. Perturbation is, therefore, not symmetric. Figure 5 shows the result when We is varied and Fr is fixed. From this figure, it is found that L/D is proportional to $We^{0.28}$. Figure 6 shows the result when Fr is varied and We is fixed. It is found that L/D is proportional to $Fr^{0.78}$. The larger Fr is, the longer the jet breakup length is. This is because the effect of gravity is smaller when Fr is larger. From the two results, we express L/D with the horizontal axis of $We^{0.28} Fr^{0.78}$ in Figure 7.

It is found that L/D is proportional to $We^{0.28} Fr^{0.78}$, and the coefficient is 2.2. Hence, L/D is expressed as

$$L/D = 2.2 We^{0.28} Fr^{0.78} \quad (16)$$

By comparison with experiment³⁾, both of the calculation result and experimental data are proportional to $We^{0.28} Fr^{0.78}$ (Fig.7). Hence the dependencies of the jet breakup length on Fr and We agree well between the MPS calculation and the experimental data. However, the coefficient 2.2 of the MPS method is a little smaller than those of the experiments for alcohol 2.5 and water 3.0.

Moreover, we analyze the jet breakup length without gravity. It is found that L/D is expressed as the following expression.

$$L/D = 7.0 We^{0.32} \quad (17)$$

We compare the result with the following Grant-Middleman's experimental correlations⁴⁾ in figure 8.

$$(\text{laminar}) \quad L/D = 19.5(We^{1/2} + 3We/Re)^{0.85} \quad (18)$$

$$(\text{turbulence}) \quad L/D = 8.51(We^{1/2})^{0.64} \quad (19)$$

These experimental correlations were obtained with horizontal jets. In this calculation, the flow must be laminar because the jet velocity is low and the continuous fluid surrounding the jet is neglected. However the calculated jet breakup lengths are shorter than the laminar correlation. The reason is the fluctuating particle motion derived from the fully Lagrangian formulation. This fluctuation may enhance the growth of the disturbance along the jet and then the breakup is accelerated. Without gravity, the initial small disturbance of the flow is dominant for the breakup.

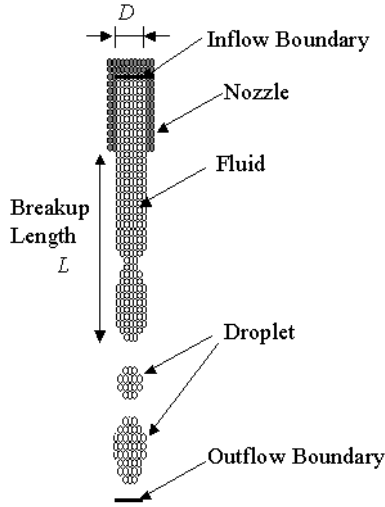


Fig.3 Calculation system

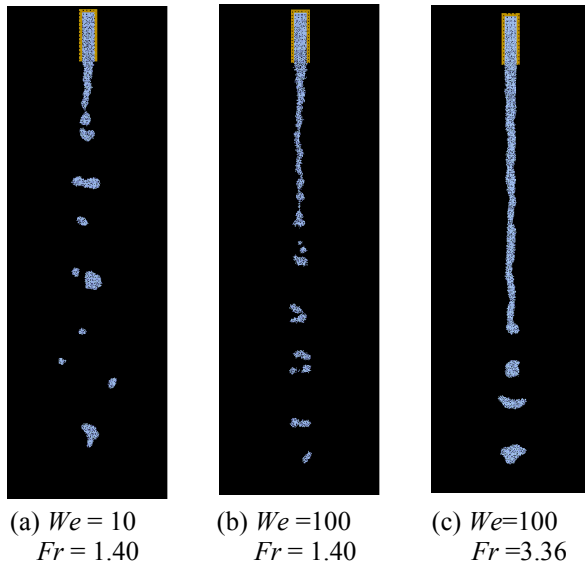


Fig.4 Calculation result of jet breakup

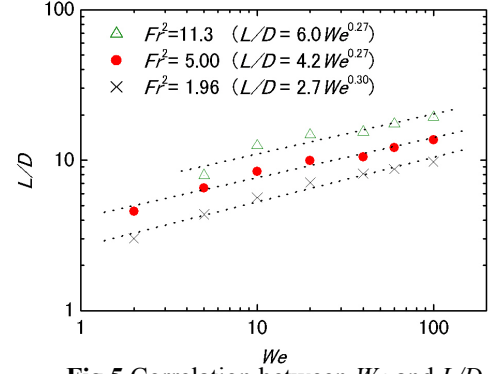


Fig.5 Correlation between We and L/D

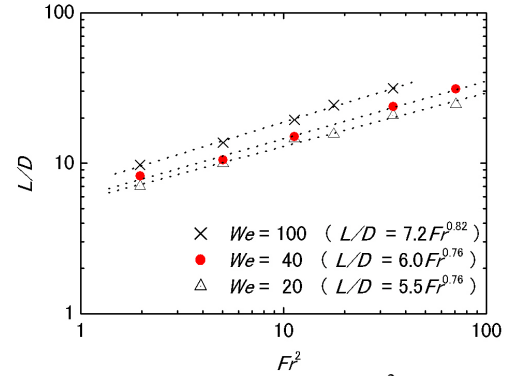


Fig.6 Correlation between Fr^2 and L/D

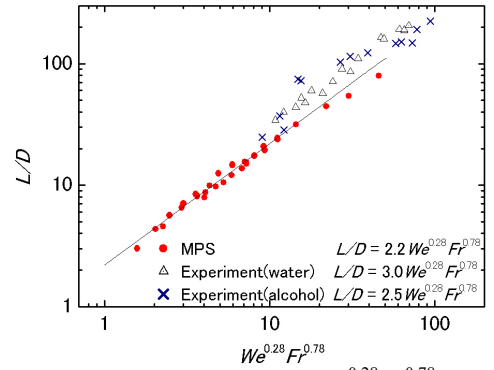


Fig.7 Correlation between $We^{0.28} Fr^{0.78}$ and L/D

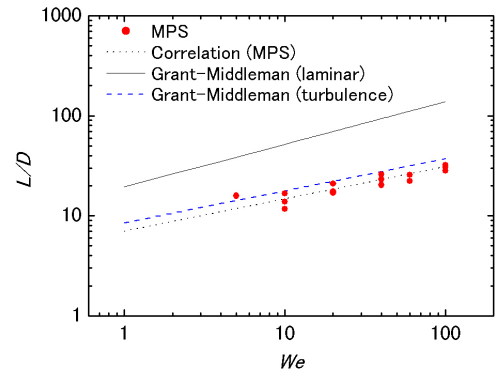


Fig.8 Correlation between We and L/D without gravity

IV. Analysis of Droplet Size Distribution

1. Calculation Condition

The condition is the same as that for the jet breakup length. The position of measuring the droplet diameter is 0.65m downward from the outlet of the nozzle. Calculations are performed with various surface tension coefficients and the flow velocities. The measuring time is 12 ~ 30 seconds. The total number of droplets is 1500 ~ 3500. Dependencies of the size distribution on We and Fr are investigated. The droplet size is defined as the equivalent diameter of a circle whose area is the number of particles in one droplet.

2. Result and Discussion

Figure 9 shows the droplet size distribution at $We = 100$ and $Fr = 1.40$. The number of measured droplets is 1721. The distribution has a peak at 6mm. It is in agreement with the Nukiyama-Tanasawa distribution⁸⁾, which has been widely used as an experimental correlation. The calculated result can also be fitted by the log-normal distribution, but not by the normal distribution.

$$\text{(Nukiyama-Tanasawa distribution)} \\ \frac{dn}{n} = Ax^\alpha \exp(-Bx^\beta) dx \quad (20)$$

$$\text{where } \alpha = 5, \beta = 1, A = 2.79 \times 10^{-3}, B = 0.833$$

$$\text{(Log-normal distribution)} \\ \frac{dn}{n} = \frac{1}{\sqrt{2\pi}\sigma} \exp\left\{-\frac{(\ln x - \mu)^2}{2\sigma^2}\right\} dx \quad (21)$$

$$\text{where } \mu = 1.97, \sigma = 0.422$$

$$\text{(Normal distribution)} \\ \frac{dn}{n} = \frac{1}{\sqrt{2\pi}\sigma} \exp\left\{-\frac{(x - \mu)^2}{2\sigma^2}\right\} dx \quad (22)$$

$$\text{where } \mu = 6.00, \sigma = 2.80$$

A typical set of parameters of the Nukiyama-Tanasawa distribution is $\alpha = 2, \beta = 1$ in experiments. The calculated distribution is correlated by $\alpha = 5, \beta = 1$, which is different from the experiments. The reason is not clarified.

The size distribution is much different is sold fragments where smaller fragments are generated more. In liquids, surface tension suppresses the number of smaller droplets. This is a qualitative explanation of the Nukiyama-Tanasawa distribution. Quantitative consideration remains in future.

In the calculated size distribution, many small droplets consisting of one particle appear. The reason is attributed to the surface tension model of the MPS method. In the past study, it was shown that the number of particles in one droplet must be large enough (about 100) to evaluate the surface tension accurately¹⁷⁾. The surface tension is calculated as zero for a single particle. These small droplets are not physical and need to ignore.

Figure 10 shows the effect of We . A smaller We leads to larger droplets because the surface tension is relatively stronger. When We is 5, two peaks emerge. This is explained as the following two mechanisms. A large

droplet is sometimes disintegrated into two half droplets and a small droplet is often generated between two large droplets.

Figure 11 shows the effect of Fr . A larger Fr leads to larger droplets. When Fr is larger, effect of gravity is smaller and the jet can keep the continuous shape for a longer distance.

The effect of the surface tension is different between two dimensions and three dimensions. In three dimensions the surface tension is stronger than that of in two dimensions. The droplet size will be larger. However, the correlations of We and Fr are the same because We and Fr are relative quantity of inertia, surface tension and gravity.

The calculation results look as involving random behavior though the MPS method has no random process in the formulation. Splashing of water was calculated and the behavior looked very similar to experimental photographs^{13, 14)}. This is a typical advantage of the particle method where grids are not necessary at all. The present study shows that liquid disintegration from a jet is not far from the real physical behavior except for small droplets of single particle.

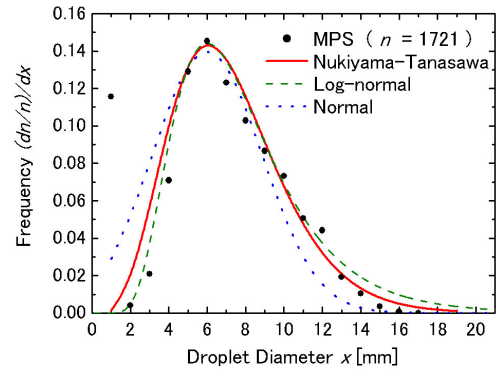


Fig.9 Droplet size distribution
($We = 100, Fr = 1.40$)

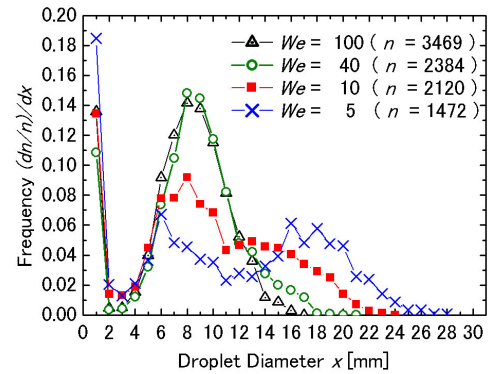


Fig.10 Effect of We ($Fr = 1.40$)

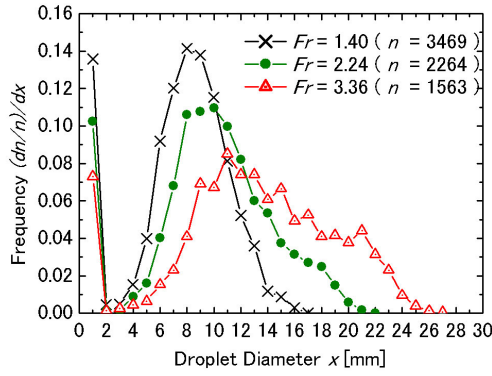


Fig.11 Effect of Fr
($We=100$)

Nomenclature

\vec{a} : gradient of particle number density
 A : constant for Nukiyama-Tanasawa distribution
 B : constant for Nukiyama-Tanasawa distribution
 D : the number of space dimensions
 d^{st} : thickness of free surface
 Fr : Froude number $Fr = \frac{U}{\sqrt{gD}}$
 \vec{g} : acceleration of gravity
 l_0 : spacing between particles in the initial configuration
 L : jet breakup length
 n : the total number of droplets
 n_i : particle number density of particle i
 n^0 : constant of the particle number density
 n_i^{st1} : particle number density for surface tension
 n_i^{st2} : particle number density for surface tension
 n_0^{st} : constant of the particle number density for surface tension
 n_0^{lccg} : constant of the particle number density for Laplacian operator
 \vec{n} : unit normal vector
 \vec{n}_x : unit vector in x-direction
 \vec{n}_y : unit vector in y-direction
 On : Ohnesorge number $On = \frac{\mu}{(\rho D \sigma)^{0.5}}$
 P : pressure
 \vec{r} : coordinates
 r : distance between particles
 r_e : radius of the interaction area
 \vec{u} : flow velocity
 U : initial jet velocity
 w : weight function
 w^{st1} : weight function for surface tension
 w^{st2} : weight function for surface tension
 We : Weber number $We = \frac{\rho U^2 D}{\sigma}$
 x : diameter of droplet
 Z : the number of space dimensions
 α : parameter for Nukiyama-Tanasawa distribution
 β : parameter for Nukiyama-Tanasawa distribution, parameter for free surface
 ϕ : arbitrary quantity
 δ : delta function

κ : curvature

λ : parameter use in Laplacian model

θ : angle

ρ : density

σ : surface tension,

constant for droplet size distribution

μ : viscosity, constant for droplet size distribution

V. Conclusions

Numerical analysis of jet breakup is performed using the MPS method in x-y two dimensions. Effects of the Weber number and the Froude number on the jet breakup length agree well with experimental data. The breakup length with gravity is from 70 to 80% of the experimental data. Jet breakup without gravity is also analyzed and the breakup length is about 25% of the experiment. This is because fluctuating motion of particles accelerates the breakup.

The size distribution of droplets after the breakup is obtained from the calculation result. It is in agreement with the Nukiyama-Tanasawa distribution which has been widely used as an experimental correlation. Effects of the Weber number and the Froude number on the size distribution are discussed.

References

- 1) Corradini, M. L., Kim, B. J. and Oh, M. D., "Vapor Explosions in Light Water Reactors: A Review of Theory and Modeling", *Progress in Nuclear Energy*, **22**, 1-117 (1988)
- 2) Ricou, F. P., and Spalding D. B., "Measurements of Entrainment by Axisymmetrical Turbulent Jets", *J. Fluid Mech.*, **11**, 21-32 (1961)
- 3) Tanasawa, Y. and Toyoda, S., "On the Atomization of Liquid Jet Issuing from a Cylindrical Nozzle", *The Technology Report of Tohoku University*, **19**, 135-156 (1955)
- 4) Grant, R. P. and Middleman, S., "Newtonian Jet Stability", *A.I.Ch.E. J.*, **12**, 669-677 (1966)
- 5) Saito, M., Sato, K. and Imahori, S., "Experimental Study on Penetration Behavior of Water Jet into Freon-11 and Liquid Nitrogen", *ANS Proc. 1988 National Heat Transfer Conf., Houston*, July 24-27, 173-183 (1988)
- 6) Park, H. S., Yamano, N., Maruyama, Y., Moriyama, K., Yang, Y. and Sugimoto, J., "Study on Energetic Fuel-Coolant Interaction in the Coolant Injection Mode of Contact," *Proc. 6th Int. Conf. Nucl. Eng. (ICONE-6)*, San Diego, May 10-15, ICONE-6091 (1998)
- 7) Kolev, N., "Multiphase Flow Dynamics 1 & 2", *Springer* (2002)
- 8) Nukiyama, S. and Tanasawa, Y., "An Experiment on

- the Atomization of Liquid” (3rd Report, On the Distribution of the Size of Droplets), *Trans. Japan Soc. Mech. Engineers*, **5**, 131-135 (1939)
- 9) Moriyama, K., Maruyama, Y. and Nakamura, H., “A Simple Evaluation Method of the Molten Fuel Amount in a Premixing Region of Fuel-Coolant Interactions”, *J. Nucl. Sci. Tech.*, **39**, 53-58 (2002)
 - 10) Vierow, K., “Development of the VESUVIUS Module – Molten Jet Breakup Modeling and Model Verification”, *Proc. OECD/CSNI Specialists Meeting on Fuel-Coolant Interactions*, Tokai, May 19-21, 541-566 (1997)
 - 11) Richard, J. G., Lenhoff, A. M. and Beris, A. N., “Dynamic Breakup of Liquid-Liquid Jets”, *Phys. Fluids*, **6**, 2640-2655 (1994)
 - 12) Richard, J. G., Beris, A. N. and Lenhoff, A. M., “Drop Formation in Liquid-Liquid Systems before and after Jetting”, *Phys. Fluids*, **7**, 2617-2630 (1995)
 - 13) Koshizuka, S., Tamako, H. and Oka, Y., “A article Method for Incompressible Viscous Flow with Fluid Fragmentation”, *Comput. Fluid Dynamics J.* **4**, 29-46 (1995)
 - 14) Koshizuka, S., and Oka, Y., “Moving-Particle Semi-Implicit Method for Fragmentation of Incompressible Fluid”, *Nucl. Sci. Eng.*, **123**, 421-434 (1996)
 - 15) Koshizuka, S., Nobe, A. and Oka, Y., “Numerical Analysis of Breaking Waves using the Moving Particle Semi-implicit Method”, *Int. J. Numer. Meth. Fluids*, **26**, 751-769 (1998)
 - 16) Ikeda, H., Koshizuka, S., Oka, Y., Park, H. S. and Sugimoto, J., “Numerical Analysis of Jet Injection Behavior for Fuel –Coolant Interaction using Particle Method”, *J. Nucl. Sci. Technol.*, **38**, 174-182 (2001)
 - 17) Nomura, K., Koshizuka, S., Oka, Y. and Obata, H., “Numerical Analysis of Droplet Breakup Behavior using Particle Method”, *J. Nucl. Sci. Technol.*, **38**, 1057-1064 (2001)
 - 18) Brackbill, J. U., Kothe, D. B. and Zemach, C., “A Continuum Method for Modeling Surface Tension”, *J. Comput. Phys.*, **100**, 335-354 (1992)
 - 19) Shirakawa, N., Horie, H., Yamamoto, Y., Okano, Y. and Yamaguchi, A., “Analysis of Jet Flows with the Two-Fluid Particle Interaction Method”, *J. Nucl. Sci. Technol.*, **38**, 729-738 (2001)
 - 20) Pilch M. and Erdman C. A., 1987, “Use of Breakup Time Data and Velocity History Data to Predict the Maximum Size of Stable Fragments for Acceleration-induced Breakup of a Liquid Drop”, *Int. J. Multiphase Flow*, **13**, No. 6, 741-757
-